Journal of the Korean Physical Society, Vol. 52, No. 4, April 2008, pp. 1206∼1210

Bond-Valence Model of Ferroelectric $PbTiO_3$

Young-Han Shin and Byeong-Joo Lee
Department of Materials Science and Engineering, Pohang University of Science and Technology, Pohang 790-784

Andrew M. Rappe*
The Makineni Theoretical Laboratories, Department of Chemistry, University of Pennsylvania, Philadelphia, Pennsylvania 19104-6323, U.S.A.

(Received 12 November 2007)

A classical potential parameterized for the reproduction of density functional calculations is used to describe the behavior of complex ferroelectric $PbTiO_3$. A scoring function is defined in terms of the energy differences and the forces of the reference structures that are generated from *ab-initio* molecular dynamics simulations with various strained lattice vectors. The elastic properties of ferroelectric $PbTiO_3$, as well as the phase transition temperature, have been improved by the addition of the strained reference structures.

PACS numbers: 77.80.-e, 02.70.Ns
Keywords: Ferroelectric, Density functional theory, Bond-valence model

I. INTRODUCTION

Ferroelectricity in perovskites has prompted wide investigation due to applications, such as nonvolatile random access memories [1–7]. When an external electric field is applied to ferroelectric materials, the polarization direction changes along the field direction and this polarization state remains after the field is turned off. In studies of the field dependence of ferroelectrics by Merz, Miller and Weinreich and Stadler [1,8,9], the nucleation rates were found to have an exponential relation to the external electric fields, which is known as Merz law. Tybell *et al.* recently observed Merz law in PZT thin films by using atomic force microscopy and showed that the size of each flipped domain could be controlled to make high-density nonvolatile random access memories [3]. However, a detailed experimental understanding of the switching process is still hampered by the difficulty in detecting the fast domain wall motion and separating the intrinsic domain wall speed from extrinsic effects. Even though density-functional theory (DFT) calculations are required for this study, they demand too many computations to observe the dynamical property of ferroelectrics.

Atomic potential models have been designed to clarify the physical phenomena that are hidden in real complex systems. These gave opportunities to approach large systems, like a moving domain wall, with available computer resources. The first model for an ionic system was the rigid ion model, sometimes called the Born model. In the rigid ion model, the ions interact with each other through the Coulomb interaction, but the polarizability of atoms is not considered in this model. Following the rigid ion model, the shell model was first developed by Dick and Overhauser to include the effect of the polarizability [10,11]. A massless spherical shell of charge $-q$ surrounds an ion of charge $(Z+q)$ and is attached to the ion by a harmonic spring. In a modified version of the shell model, the radius of the shell is a variable.

Recently, another potential model has been suggested from a completely different idea – the inverse relation between the bond valence (or the bond order) and the bond length. This empirical relation was developed from an inorganic experimental database and its parameters were summarized by Brown *et al.* [12–14]. The bond-valence model was successfully applied to $PbTiO_3$ [15–17]. Here, we are going to show how the potential parameters are optimized from the first-principles reference structures. We added more reference structures to consider the elastic properties, which enabled us to run molecular dynamics simulations at a constant stress.

II. BOND-VALENCE MODEL AND OPTIMIZATION OF PARAMETERS

The bond-valence model is based on the empirical database relating the bond lengths to the bond valences [12]. We create an interatomic potential from bond-valence concepts by adding several energy terms:

$$E_{bv} = E_c + E_r + E_b + E_a. \quad (1)$$

*E-mail: rappe@sas.upenn.edu

Table 1. Optimized potential parameters of the bond-valence model potential function. The angle potential parameter k is 1.43 meV/(°)^2.

					$B_{\beta\beta'}$ (Å)		
β	$r^0_{\beta O}$	$C_{\beta O}$	q_β (e)	S_β (eV)	Pb	Ti	O
Pb	1.969	5.5	1.419	0.013	-	2.224	1.686
Ti	1.804	5.2	1.036	0.223	2.224	-	1.201
O	-	-	–0.818	0.702	1.686	1.201	1.857

E_c is a Coulombic potential that is similar to the one in the Born model with charges of ions and these partial charges are fitting parameters. E_r is a short-range potential with only a repulsive term:

$$E_r = 8\varepsilon \sum_{\beta=1}^{3}\sum_{i=1}^{N_\beta}\sum_{\beta'=1}^{3}\sum_{i'=1}^{N_{\beta'}}\left(\frac{B_{\beta\beta'}}{r_{ii'}^{\beta\beta'}}\right)^{12}. \quad (2)$$

The relation between the bond length and the bond valence is expressed with E_b as

$$E_b = \sum_{\beta=1}^{3} S_\beta \sum_{i=1}^{N_\beta}\left(V_{i\beta} - V_\beta\right)^2, \quad (3)$$

where

$$V_{i\beta} = \sum_{\beta'=1}^{3}\sum_{i'(n.n.)}\left(\frac{r_o^{\beta\beta'}}{r_{ii'}^{\beta\beta'}}\right)^{C_{\beta\beta'}} \quad (4)$$

is the bond valence of the ith atom of type β. β is the index for Pb, Ti and O ions and N_β is the number of β ions. V_β is the desired atomic valence of the β ion and $r_{ii'}^{\beta\beta'}$ is the distance between the ith β ion and the i'th β' ion. The angle potential E_a is introduced to correct for the octahedral tilt at high temperatures.

Reference structures are required to optimize the potential parameters. We generate the reference structures by using *ab-initio* molecular dynamics simulations as implemented in VASP [18,19]. The local density approximation was used for exchange and correlation and the projector augmented wave potential was used for the pseudopotential [20]. The plane waves were included in the wave functions up to 500 eV. A 2 × 2 × 2 supercell was used to consider the octahedral tilt angle and 14 k points were used for the k space integration in the irreducible Brillouin zone. The optimized cell parameters of the tetragonal $PbTiO_3$ are a = 3.87 Å and c = 4.05 Å. In addition to the *ab-initio* molecular dynamics simulations, we performed static *ab-initio* calculations of the relaxed atomic coordinates with a series of strained lattice vectors. This served as a way to check whether this information would be helpful in adjusting the elastic properties.

We used the simulated annealing algorithm to find the optimized potential parameters. The scoring function, P, is defined as

$$P = \frac{1}{N_s}\sum_{i=1}^{N_s}\left(w_E\Delta E_i + w_F\Delta F_i\right), \quad (5)$$

where

$$\Delta E_i = \left|(E^i_{DFT} - E^0_{DFT}) - (E^i_{bv} - E^0_{bv})\right|, \quad (6)$$

$$\Delta F_i = \sum_{j=1}^{N_a}\sum_{m=1}^{3}\left|F^{i,j,m}_{DFT} - F^{i,j,m}_{bv}\right|. \quad (7)$$

N_s is the number of reference structures and N_a is the number of atoms. E^0_{DFT} and E^0_{bv} are the minimal DFT and the model potential energies among all the reference structures, respectively. The upper indices i, j and m, respectively, denote the reference structures, atoms and dimensions. w_E is the weight for the energy term and w_F is the weight for the force term. These weights must be determined carefully to achieve optimal parameters.

Since the lattice constants are underestimated in the local density approximation, Brown's empirical parameters $r_0^{\beta\beta'}$ and $C_{\beta\beta'}$ need to be adjusted. This is useful for generating the potential parameters of other ferroelectrics, where the empirical parameters are not known. We fix $C_{\beta\beta'}$ to the empirical values ($C_{\mathrm{PbO}} = 5.5$ and $C_{\mathrm{TiO}} = 5.2$) and express $r_0^{\beta\beta'}$ in terms of the displacements of ions (δ_{Pb}, δ_{Ti}, δ_{O} and $\delta_{\mathrm{O}'}$) and the lattice constants a and c (Figure 1):

$$r_0^{\mathrm{PbO}} = \left[\frac{1/2}{\left((\frac{a}{2})^2 + (\frac{c}{2} - \delta_{\mathrm{Pb}} - \delta_{\mathrm{O}})^2\right)^{-\frac{C_{\mathrm{PbO}}}{2}} + \left((\frac{a}{2})^2 + (\frac{c}{2} + \delta_{\mathrm{Pb}} + \delta_{\mathrm{O}})^2\right)^{-\frac{C_{\mathrm{PbO}}}{2}} + \left(2(\frac{a}{2})^2 + (\delta_{\mathrm{Pb}} + \delta_{\mathrm{O}'})^2\right)^{-\frac{C_{\mathrm{PbO}}}{2}}}\right]^{1/N_{\mathrm{PbO}}} = 1.969 \quad (8)$$

$$r_0^{\mathrm{TiO}} = \left[\frac{4}{\left(\frac{c}{2} - \delta_{\mathrm{Ti}} - \delta_{\mathrm{O}'}\right)^{-\frac{C_{\mathrm{TiO}}}{2}} + 4\left((\frac{a}{2})^2 + (\delta_{\mathrm{Ti}} + \delta_{\mathrm{O}})^2\right)^{-\frac{C_{\mathrm{TiO}}}{2}} + \left(\frac{c}{2} - \delta_{\mathrm{Ti}} - \delta_{\mathrm{O}'}\right)^{-\frac{C_{\mathrm{TiO}}}{2}}}\right]^{1/N_{\mathrm{TiO}}} = 1.804, \quad (9)$$

where $\delta_{\mathrm{Pb}} = 0.234$ Å, $\delta_{\mathrm{Ti}} = 0.096$ Å, $\delta_{\mathrm{O}} = -0.188$ Å and $\delta_{\mathrm{O}'} = -0.137$ Å from the first-principles calculation. The calculated $r_0^{\beta\beta'}$ parameters are slightly smaller than the

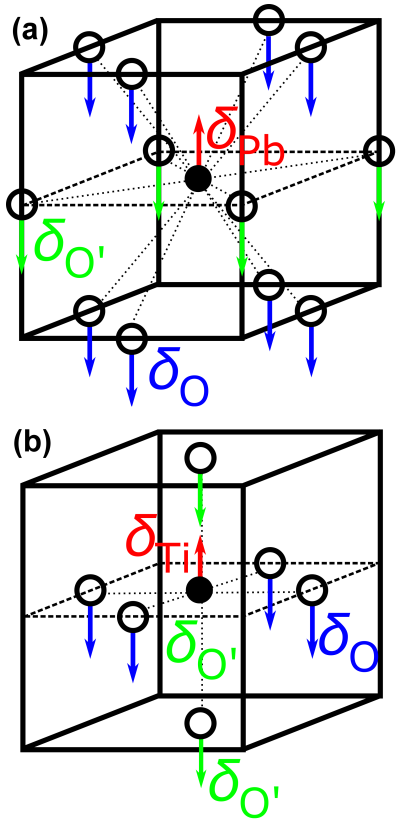

Fig. 1. Nearest-neighbor oxygen ions around Pb and Ti ions. (a) A solid circle designates a Pb ion and 12 oxygen ions (open circles) are located at the same distance from the Pb ion. Arrows show the displacement of ions in the ferroelectric state. (b) A solid circle designates a Ti ion and 6 oxygen ions (open circles) are located at the same distance from the Ti ion.

experimental values ($r_0^{\mathrm{PbO}} = 2.044$ and $r_0^{\mathrm{TiO}} = 1.806$). The optimized potential parameters are summarized in Table 1 and the energy difference between DFT and the bond-valence model is shown in Figure 2. The average of the energy difference is 0.0095 eV per atom with a standard deviation of 0.0057 eV per atom.

III. ELASTICITY OF TETRAGONAL $PbTiO_3$

The elastic energy per unit volume is given by

$$E = \frac{1}{2}\sum_{i,j} C_{ij}\epsilon_i\epsilon_j. \tag{10}$$

C_{ij} is an element of the 6×6 symmetric stiffness tensor $\mathbf{C}$ and ϵ_i is a strain component following the Voigt notation [21]:

$$\begin{pmatrix} \epsilon_1 & \epsilon_6 & \epsilon_5 \\ \epsilon_6 & \epsilon_2 & \epsilon_4 \\ \epsilon_5 & \epsilon_4 & \epsilon_3 \end{pmatrix} = \begin{pmatrix} \epsilon_{11} & 2\epsilon_{12} & 2\epsilon_{13} \\ 2\epsilon_{12} & \epsilon_{22} & 2\epsilon_{23} \\ 2\epsilon_{13} & 2\epsilon_{23} & \epsilon_{33} \end{pmatrix}. \tag{11}$$

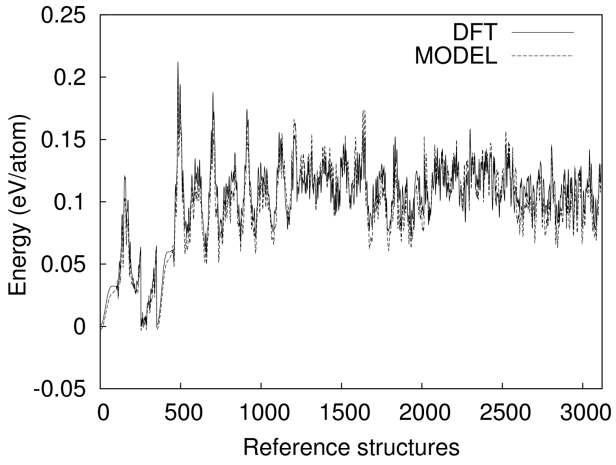

Fig. 2. Comparison of the energy difference between the DFT and the model potential. Around 3200 reference structures with strained lattice vectors were used to optimize the potential parameters.

$\epsilon_{\alpha\beta}$ is defined as

$$\epsilon_{\alpha\beta} = \frac{1}{2}\left(\frac{\partial u_\alpha}{\partial x_\beta} + \frac{\partial u_\beta}{\partial x_\alpha}\right), \tag{12}$$

where $\mathbf{u}$ is a displacement vector. By introducing a matrix $\mathbf{T}$ and γ, we can write ϵ as

$$\epsilon = \gamma\mathbf{T}. \tag{13}$$

For a tetragonal structure, the stiffness tensor $\mathbf{C}$ is as simple as

$$\mathbf{C} = \begin{pmatrix} C_{11} & C_{12} & C_{13} & 0 & 0 & 0 \\ C_{12} & C_{11} & C_{13} & 0 & 0 & 0 \\ C_{13} & C_{13} & C_{33} & 0 & 0 & 0 \\ 0 & 0 & 0 & C_{44} & 0 & 0 \\ 0 & 0 & 0 & 0 & C_{44} & 0 \\ 0 & 0 & 0 & 0 & 0 & C_{66} \end{pmatrix}, \tag{14}$$

and the elastic energy is

$$\begin{aligned} E &= \frac{1}{2}C_{11}\left(\epsilon_1^2+\epsilon_2^2\right) + \frac{1}{2}C_{33}\epsilon_3^2 + \frac{1}{2}C_{44}\left(\epsilon_4^2+\epsilon_5^2\right) \\ &+\frac{1}{2}C_{66}\epsilon_6^2 + C_{12}\epsilon_1\epsilon_2 + C_{13}\left(\epsilon_1\epsilon_3+\epsilon_2\epsilon_3\right) \\ &= \frac{1}{2}C_{11}\left(\epsilon_{11}^2+\epsilon_{22}^2\right) + \frac{1}{2}C_{33}\epsilon_{33}^2 \\ &+2C_{44}\left(\epsilon_{23}^2+\epsilon_{13}^2\right) + 2C_{66}\epsilon_{12}^2 + C_{12}\epsilon_{11}\epsilon_{22} \\ &+C_{13}\left(\epsilon_{11}\epsilon_{33}+\epsilon_{22}\epsilon_{33}\right). \end{aligned} \tag{15}$$

The elements of the elastic stiffness tensor are obtained by determining proper $\mathbf{T}$ tensors (see Table 2) [22] and they show good agreement with experiments [23,24].

When the model potential energies with the original parameter set in Ref. 14 is calculated with the six strain tensors in Table 2, the energy differences between DFT and the model calculations for **the** $\mathbf{T}^{(11)}$, $\mathbf{T}^{(13)}$ and

Table 2. Strain tensors, elastic energies and the elastic stiffness tensor **C**.

T	ϵ	E	Elements of the stiffness tensor
$\mathbf{T}^{(11)}=\begin{pmatrix}1&0&0\\0&0&0\\0&0&0\end{pmatrix}$	$\begin{pmatrix}\gamma&0&0\\0&0&0\\0&0&0\end{pmatrix}$	$\frac{1}{2}C_{11}\gamma^2$	$C_{11}=\frac{\partial^2 E}{\partial\gamma^2}$
$\mathbf{T}^{(33)}=\begin{pmatrix}0&0&0\\0&0&0\\0&0&1\end{pmatrix}$	$\begin{pmatrix}0&0&0\\0&0&0\\0&0&\gamma\end{pmatrix}$	$\frac{1}{2}C_{33}\gamma^2$	$C_{33}=\frac{\partial^2 E}{\partial\gamma^2}$
$\mathbf{T}^{(44)}=\begin{pmatrix}0&0&1\\0&0&0\\1&0&0\end{pmatrix}$	$\begin{pmatrix}0&0&\gamma\\0&0&0\\\gamma&0&0\end{pmatrix}$	$2C_{44}\gamma^2$	$C_{44}=\frac{1}{4}\frac{\partial^2 E}{\partial\gamma^2}$
$\mathbf{T}^{(66)}=\begin{pmatrix}0&1&0\\1&0&0\\0&0&0\end{pmatrix}$	$\begin{pmatrix}0&\gamma&0\\\gamma&0&0\\0&0&0\end{pmatrix}$	$2C_{66}\gamma^2$	$C_{66}=\frac{1}{4}\frac{\partial^2 E}{\partial\gamma^2}$
$\mathbf{T}^{(12)}=\begin{pmatrix}1&0&0\\0&1&0\\0&0&0\end{pmatrix}$	$\begin{pmatrix}\gamma&0&0\\0&\gamma&0\\0&0&0\end{pmatrix}$	$C_{11}\gamma^2+C_{12}\gamma^2$	$C_{12}=\left(\frac{\partial^2 E}{\partial\gamma^2}-2C_{11}\right)/2$
$\mathbf{T}^{(13)}=\begin{pmatrix}1&0&0\\0&0&0\\0&0&1\end{pmatrix}$	$\begin{pmatrix}\gamma&0&0\\0&0&0\\0&0&\gamma\end{pmatrix}$	$\frac{1}{2}C_{11}\gamma^2+\frac{1}{2}C_{33}\gamma^2+C_{13}\gamma^2$	$C_{13}=\left(\frac{\partial^2 E}{\partial\gamma^2}-C_{11}-C_{33}\right)/2$

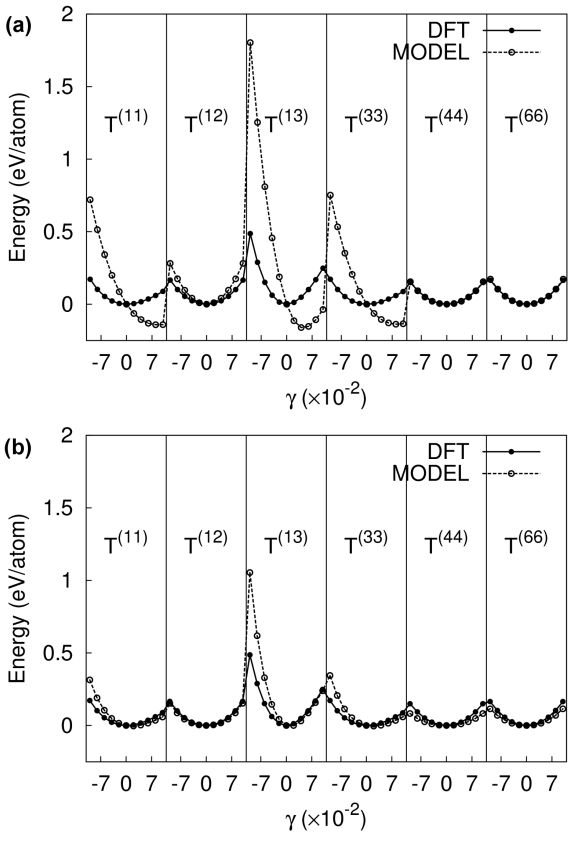

Fig. 3. Comparison between the DFT calculation and the model potential with (a) the potential parameters in Ref. 14 and (b) the potential parameters in this study. γ is a scalar measure of the magnitude and sign of the strain ϵ in Eq. (13).

Table 3. Elastic stiffness constants for $PbTiO_3$ in this study compared with the literature values in units of GPa.

	This study	Literature values		
	DFT	Ref. 23[a]	Ref. 24[a]	Ref. 25[b]
C_{11}	290 ± 2	237 ± 3	235 ± 3	133
C_{33}	101 ± 1	90 ± 10	105 ± 7	93
C_{44}	62 ± 0	69 ± 1	65 ± 1	80
C_{66}	103 ± 0	104 ± 1	104 ± 1	93
C_{12}	117 ± 0	90 ± 5	101 ± 5	85
C_{13}	92 ± 0	100 ± 10	99 ± 8	89

[a]Single-crystal Brillouin measurements.
[b]Lattice dynamics calculations using a rigid ion model.

$\mathbf{T}^{(33)}$ strain tensors are very large (Figure 3(a)). Thus, the system with the original parameter set will be unstable at those strains. However, the new parameter set in Table 1 gives good agreement between the energy difference from the DFT calculations and the energy difference from the bond-valence potential model (Figure 3(b)). The previously reported potential parameters are good for constant temperature molecular dynamics simulations at room temperature. However, the phase transition temperature of the potential parameter set is smaller than the experimental one by about 200 K. Also this potential parameter set is not good for constant stress simulations because the supercell breaks at finite temperatures. These problems can be solved by adding more reference structures with a variety of lattice constants. The tetragonal-to-cubic phase transition temperature from the new parameter set in Table 1 is

$\sim$700 K, which is much closer to the experimental value than the value obtained by using the old parameters in Ref. 14. Also, the new parameter set enables us to perform constant pressure simulations because it considers energies with different cell shapes.

IV. CONCLUSIONS

We introduced an atomic potential model based on a physical property (the inverse relation between the bond length and the bond valence) for $PbTiO_3$. To optimize the parameters of this potential model, we used the simulated annealing global optimization method. A scoring function was generated in terms of the energy differences and the forces of reference structures, which were obtained from the DFT calculations. From the lattice constants and the displacements of ions, we could determine $r_o^{\beta\beta'}$. The other potential parameters were obtained by using the simulated annealing method to minimize the scoring function. By adding the strained reference structures, we were able to reproduce the elastic properties of $PbTiO_3$ from DFT calculations in the atomic potential model.

ACKNOWLEDGMENTS

This work was supported by the Brain Korea 21 Project and by the U.S. Department of Energy Grant No. DE-FG02-07ER46431.

REFERENCES

[1] R. C. Miller and G. Weinreich, Phys. Rev. **117**, 1460 (1960).
[2] M. E. Lines and A. M. Glass, *Principles and Applications of Ferroelectrics and Related Materials* (Clarendon Press, Oxford, 1977).
[3] T. Tybell, P. Paruch, T. Giamarchi, and J.-M. Triscone, Phys. Rev. Lett. **89**, 097601 (2002).
[4] T. Morita and Y. Cho, J. Korean Phys. Soc. **46**, 10 (2005).
[5] M. Choi, D. H. Kim and C. H. Park, J. Korean Phys. Soc. **49**, S481 (2006).
[6] S. Nakashima, K.-Y. Yun, Y. Nakamura and M. Okuyama, J. Korean Phys. Soc. **51**, 882 (2007).
[7] J. Y. Son, S. Min, C. H. Kim, B. G. Kim and J. H. Cho, J. Korean Phys. Soc. **51**, 655 (2007).
[8] W. J. Merz, Phys. Rev. **95**, 690 (1954).
[9] H. L. Stadler and P. J. Zachmanidis, J. Appl. Phys. **34**, 3255 (1963).
[10] B. G. Dick and A. W. Overhauser, Phys. Rev. **112**, 90 (1958).
[11] M. Sepliarsky and R. E. Cohen, AIP Conf. Proc. **626**, 36 (2002).
[12] I. Brown and R. Shannon, Acta Cryst. A **29**, 266 (1973).
[13] I. Brown and K. K. Wu, Acta. Cryst. B **32**, 1957 (1976).
[14] I. D. Brown, in *Structure and Bonding in Crystals II*, edited by M. O'Keeffe and A. Navrotsky (Academic Press, New York, New York, 1981), p. 1.
[15] I. Grinberg, V. R. Cooper and A. M. Rappe, Nature **419**, 909 (2002).
[16] Y.-H. Shin, V. R. Cooper, I. Grinberg and A. M. Rappe, Phys. Rev. B **71**, 054104 (2005).
[17] Y.-H. Shin, I. Grinberg, I.-W. Chen and A. M. Rappe, Nature **449**, 881 (2007).
[18] G. Kresse and J. Hafner, Phys. Rev. B **47**, 558 (1993).
[19] G. Kresse and J. Furthmuller, Phys. Rev. B **54**, 11169 (1996).
[20] G. Kresse and D. Joubert, Phys. Rev. B **59**, 1758 (1999).
[21] J. F. Nye, *Physical properties of crystals* (Oxford University Press, Oxford, 1989).
[22] M. Finnis, *Interatomic forces in condensed matter* (Oxford University Press, New York, 2003).
[23] A. G. Kalinichev, J. D. Bass, B. N. Sun and D. A. Payne, J. Mater. Res. **12**, 2623 (1997).
[24] Z. Li, M. Grimsditch, X. Xu and S.-K. Chan, Ferroelectrics **141**, 313 (1993).
[25] J. D. Freire and R. S. Katiyar, Phys. Rev. B **37**, 2074 (1988).